JOURNAL OF SCIENCE
SAKARYA UNIVERSITY

Sakarya University Journal of Science

ISSN 1301-4048 | e-ISSN 2147-835X | Period Bimonthly | Founded: 1997 | Publisher Sakarya University | http://www.saujs.sakarya.edu.tr/

Title: Thermo-Hydraulic Effects of Vortex Generator Pairs in A Crossflow Channel With A Transverse-Jet Flow

Authors: Besir Kok
Recieved: 2019-04-29 13:53:41

Accepted: 2019-05-21 00:45:52

Article Type: Research Article
Volume: 23
Issue: 5
Month: October
Year: 2019
Pages: 942-963

How to cite
Besir Kok; (2019), Thermo-Hydraulic Effects of Vortex Generator Pairs in A Crossflow Channel With A Transverse-Jet Flow. Sakarya University Journal of Science, 23(5), 942-963, DOI: 10.16984/saufenbilder.558877
Access link
http://www.saujs.sakarya.edu.tr/issue/44066/558877

Sakarya University Journal of Science 23(5), 942-963, 2019

Thermo-hydraulic effects of vortex generator pairs in a crossflow channel with a transverse-jet flow

Besir Kok[1]

Abstract

The use of passive obstacles to control the hydraulic and thermal behavior of fluids is an application in many industrial mechanisms. In this study, flow and thermal oscillation behaviors in a crossflow channel with a transverse jet flow were investigated numerically. Passive vortex generator(VG) pairs with different geometric properties were used in the test channel and their thermo-hydraulic effects in the active mixing zone were discussed. In addition, nine boundary conditions, which are the function of velocity and temperature, have been applied to the computational domain. The results showed that VG pairs with different geometric properties do not provide an effective improvement in thermal mixing behavior, but they are very successful in removing thermal oscillations from the channel walls. Momentum and temperature differences between cross flow and jet flow are the secondary parameters of the study. When the jet velocity was gradually increased by keeping the crossflow rate constant, improvements in thermal mixing performance were observed but in this case, it was also seen that thermal oscillations reached the channel walls. As the jet temperature increased, a decrease in thermal mixing performance was observed due to the increased hot fluid dominance in the duct.

Keywords: Transverse jet, Crossflow, Thermal mixing, LES, Vortex generator.

1. INTRODUCTION

During the mixing of fluids at different temperatures, temperature oscillations occur in the mixing zone due to the non-homogeneous thermal mixing. These oscillations may cause thermal stresses on surrounding surfaces of the fluid at certain frequencies. During long working cycles, these stresses occurring on the material surface may cause cracks. Such cracks in industrial mechanisms may cause significant disruptions in the operation of the system. Leakages from such cracks in industrial systems such as nuclear power plants can cause extremely dangerous consequences for human and environmental health. During the operation of nuclear power plants, there have been many cracks due to the thermal stress that has been detected so far. For instance, a number of cracks were found in the connection pipes of the heat exchanger in the central chamber of the Tsuruga-2 PWR (Japan) nuclear power plant, due to thermal stresses in 1999. Sodium leaks were detected in the purification cycle of the primary circuit of the BN - 600 (Russia) reactor in 1993. Metallurgical analysis showed that the problem

*Corresponding Author: besirkok@gmail.com (B. Kok)
[1] Firat University, Technical Vocational School, Elazığ, TURKEY. ORCID: 0000-0001-7241-952X

was caused by the temperature fluctuations occurring during the mixing of hot and cold sodium[1]. This kind of cracks observed in many industrial applications, particularly in nuclear power plants, led researchers to study on this subject.

Sakai et al. [2] made numerical modeling of angled jet flow in a crossflow channel to examine the cooling effect of the film on the turbine blades. Large Eddy Simulation (LES) turbulence model was used in the analysis. Crossflow and jet velocity ratios are the main parameters of the study. They analyzed the effects of this ratio on jet behavior with film cooling effectiveness and jet trajectory graphics. The results showed that the vertical structure was significantly affected by the rate of velocity. Deng et al. [3], performed a detailed numerical study on shock vector control-SVC in a non-permanent three-dimensional cross flow. Standard k-ε, Realizable k-ε, k-ω, and LES turbulence models are given in this study. The results showed that LES simulations were more successful in solving non-permanent characteristics of the flow. Liu et al. [4] studied the flow and mixing characteristics of a transverse-jet flow in a supersonic crossflow. In the analysis, LES was used as a turbulence model and the results were verified for comparison with several different numerical methods. LES simulations were confirmed by available experimental data. Chuang et al. [5,6] investigated experimentally the thermal mixing and stripping behavior in a T-junction flow. The Branch flows were positioned at 90 and 45 angles to the main flow. PSD graphs were used to analyze whether the thermal oscillations occurring in the mixture zone create a risk of thermal stress. It was analyzed whether or not the reverse flow conditions occurred in the channel by using the momentum data obtained. McGuinn et al. [7] examined the heat transfer characteristics of six parallel slot jets in a crossflow which can be controlled separately. In the experiment, a system which can detect hot points dynamically and adaptive cooling is used. The jet Reynolds numbers and the distance between the jet and the

The effects of temperature and momentum difference between jets on flow and thermal mixing behaviors are the secondary parameters of these studies. Some of the experimental studies impact plates are variable. The results showed that the parameters chosen were highly effective on heat transfer. Wang et al. [8,9] experimentally investigated the heat transfer characteristics of jet flow impinging on a heated plate in a crossflow channel. In the experiments, vortex generators(VG) in different geometries were placed in a rectangular test channel. The results show that the VG significantly increase heat transfer. Furthermore, the different geometric ratios of these VGs also affect the heat transfer in all cases. Compared to triple-crossed VG, rectangular VG was found to provide a more heat transfer improvement. As the crossflow flow rate increased, VG was found to significantly affect the heat transfer.

The regions where thermal oscillations are generally seen in industrial mechanisms are T-junctions. When the main pipe/channel flow and the secondary flow connected therein are at different temperatures, cracks can be seen as described above. There are many studies in the literature that demonstrate different thermophysical dynamics in T-junctions. In these studies, the researchers have analyzed whether the temperature oscillations in this region constitute thermomechanical threats. In order to understand this, Power Spectral Density (PSD) graphics are generally considered. These graphs provide information on the frequency and amplitude of the current temperature oscillation[10–15].

Kok et al. have made numerical and experimental studies on the thermal mixing of fluids at different temperatures in confined channels. In these studies, they used two types of jet models, mainly parallel and co-axial. The thermal mixing performance of the fluid in the channel was analyzed with the help of Mixing Index (MI) graphs. In addition, PSD graphs were obtained in order to determine whether the current temperature fluctuations posed a risk of thermal stress. It has been determined whether the thermal oscillations have reached the channel walls by using isotherms. They used velocity profiles to evaluate the turbulence behaviors of jet flows.

have examined the inclination angle of a shallow test channel and the effects of the square and circular passive barriers used in these channels. In another study, an artificial neural network

algorithm was developed using the available experimental data and estimates were made about the parameters not tested. Porous and sequential types of barriers were used in a square cross-section test channel. Large Eddy Simulation (LES) turbulence model was used for numerical modeling of these studies. Experimental data were obtained by using different experimental setups[16–23].

The above literature survey on the effects of temperature oscillations on the mechanisms shows that there are many aspects of this subject. The above literature summary shows how different aspects of this issue are addressed. Every parameter that can be effective on the temperature oscillations in the mixing zone is carefully examined by the researchers. Thermal oscillations occurring in a crossflow are the most common occurrences in industrial applications. In this study, the flow and thermal mixing characteristics of a transverse-jet flow in a crossflow were investigated numerically. LES turbulence model was used with WALE subgrid-scale model to simulate flow area. In the simulations, vortex generators pairs with different geometric properties were used to improve the thermal mixing efficiency in the mixing zone. The effects of these VGs on flow, thermal mixing behavior and pressure drop in the channel have been extensively discussed. Temperature and momentum differences between cross flow and jet flow are the secondary parameters of the study.

2. COMPUTATIONAL STUDY

Accurate analysis of the thermodynamic and dynamic characteristics of thermal mixing problems is very complicated. Since the sudden temperature oscillations in the mixing zone are random, they are difficult to predict. Therefore, such problems are not problems in which the average temperature oscillation behaviors are examined in large geometries. On the contrary, these are problems in which local behavior is examined in certain sections. As explained above, the cases in which thermal mixing are observed in industrial mechanisms are generally T connections. Therefore, in this study, the flow and thermal mixing behaviors of a jet flow positioned transversely in a cross flow were investigated numerically.

Table 1. Boundary conditions of crossflow and jet flow

	T_j (K)	T_c (K)	U_j (m/s)	U_c (m/s)	Re_j	Re_c
Case 1	318	298	0.5	0.1	8305	13427
Case 2	338	298	0.5	0.1	11316	13427
Case 3	358	298	0.5	0.1	14539	13427
Case 4	318	298	0.75	0.1	12458	13427
Case 5	338	298	0.75	0.1	16974	13427
Case 6	358	298	0.75	0.1	21802	13427
Case 7	318	298	1	0.1	16610	13427
Case 8	338	298	1	0.1	22633	13427
Case 9	358	298	1	0.1	29069	13427

For this purpose, a test channel measuring 15D x 10D x 50D was modeled. Water is used as working fluid in the channel and the jet provides hot fluid to the crossflow channel. In this study, the momentum and temperature values of the crossflow are kept constant while the temperature and momentum values of the jet flow velocities are gradually increased. Detailed information on crossflow and jet flow boundary conditions are given in Table 1. As shown, there are 9 boundary conditions which are the function of momentum and temperature. As seen in Figure 1, passive Vortex Generator (VG) pairs are placed in the channel. These VGs are two types, Rectangular and Delta, which are shown in Figure 2. When the numerical studies conducted in the past[24] regarding the thermal mixing are examined, it can

be seen that the steady-state studies do not catch the turbulence characteristic.

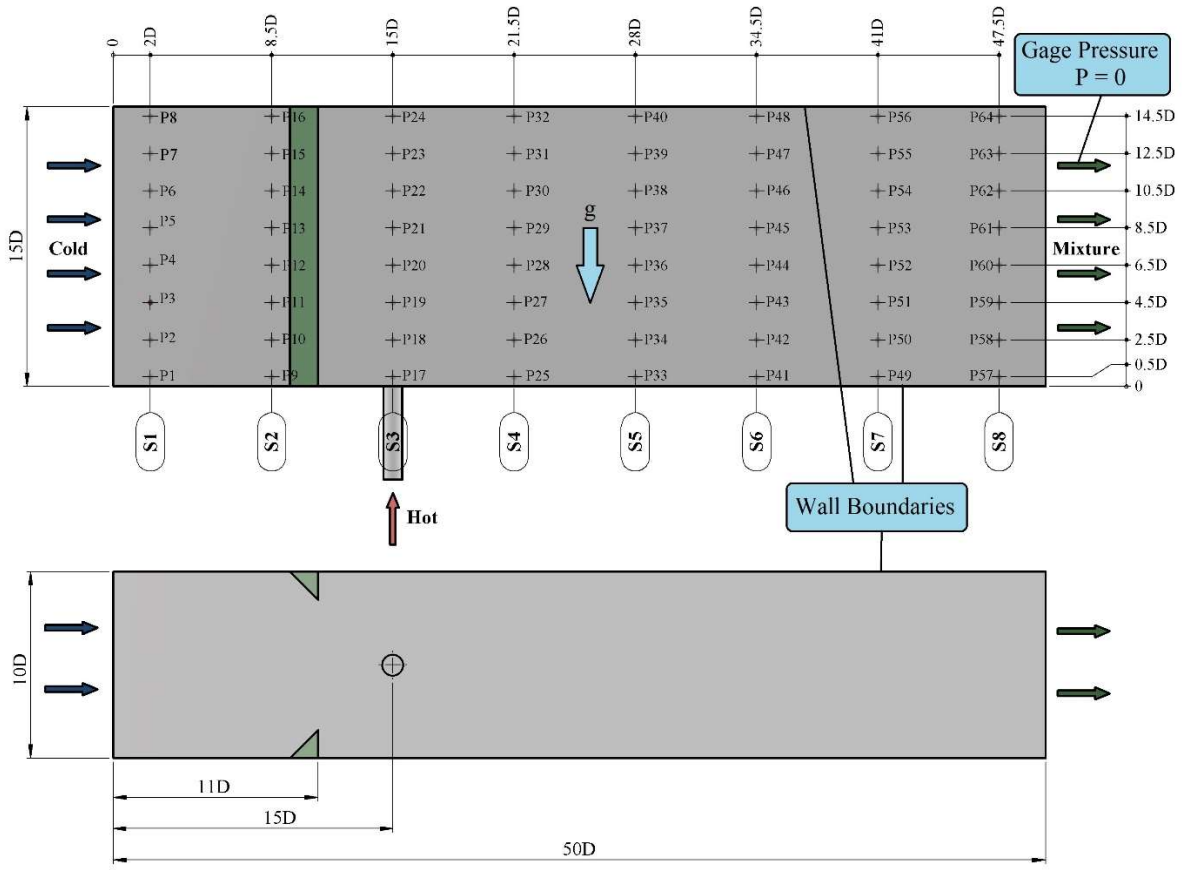

Figure 1. Computational domain and measurement points

In such analyzes, point data is difficult to detect, so the average temperature values over time should be compared. In the literature, it was seen that the LES turbulence model gave quite healthy results compared with experimental findings. Therefore, the LES turbulence model was used for modeling the flow area. In the analyzes, the permanent characteristics of the fluid were solved using the k-ε turbulence model and the fully developed flow conditions were obtained. Then, time-dependent flow conditions were obtained by using the LES turbulence model. Solutions were made for 4 seconds flow time and the data were collected at 100 Hz frequency.

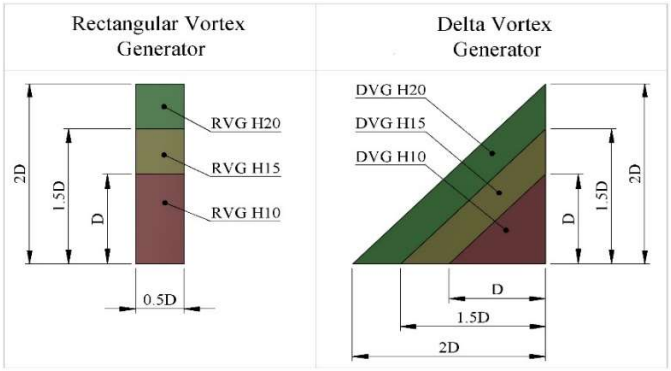

Figure 2. Dimensions of vortex generators

Time steps were defined as 0.01s in transient calculations and 20 iterations were made for each time step. The residuals drop below 8 $x10^{-5}$ after 20 iterations. Courant number is under 0.26 in the effective mixing region for all cases. Mass flow boundary conditions are used for both crossflow and the jet inlet. Wall boundaries were chosen for all the channel walls and pressure outlet boundary condition was defined in the exit of the channel (see Figure 1).

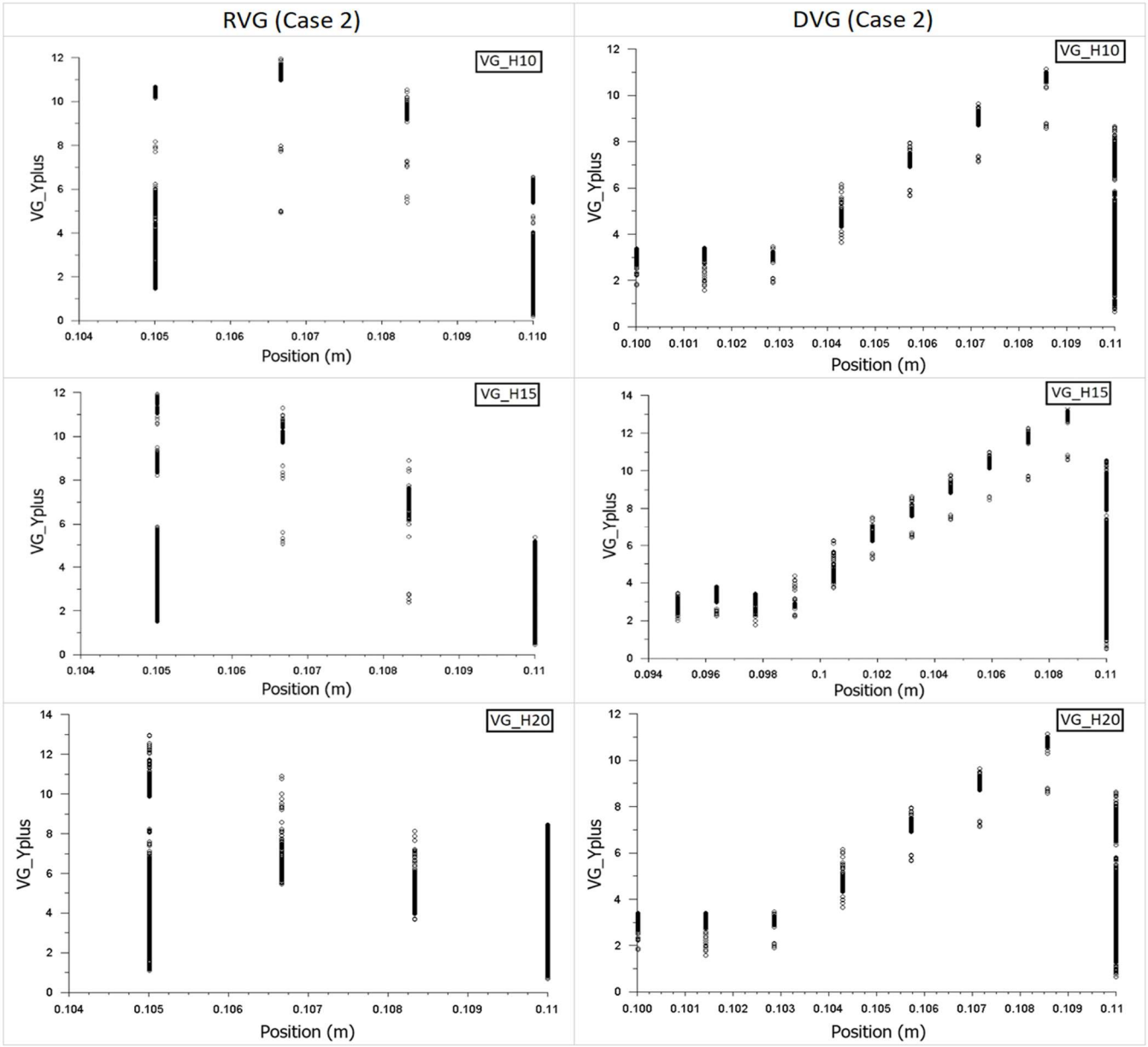

Figure 3. y+ values of wall boundaries for vortex generator pairs

In the test channel, turbulence is generated by both vortex generator pairs and flow shear. For the turbulence produced by the passive obstacles (VG), the y + value must convenient in order to capture the transition from the viscous layer to the developed layer with the appropriate turbulent energy transfer. The y + values for the present study is given at Figure 3 and as it is seen from the figure y+ values are under 14 for all cases.

2.1.Mesh Structure

ANSYS Meshing 15.0 software was used to create the mesh structure of the determined

models which are given in Figure 4. The elements must be close to the cubic structure so that the formed mesh structure is suitable for LES simulations. Since small fluctuations are modeled in the LES model, the mesh elements should be as small as possible. However, elements of appropriate sizes must be selected, since the very small dimensions of the elements will extend the calculation time.

Taylor Microscale (TMS) scale was used to determine the correct size of the elements that would not negatively affect the results of the analysis. TMS is often used in the literature in LES analyzes to characterize turbulent fluid flow. Taylor Microscale is an intermediate length scale that gains importance when fluid viscosity significantly affects the movement of turbulence vortices.

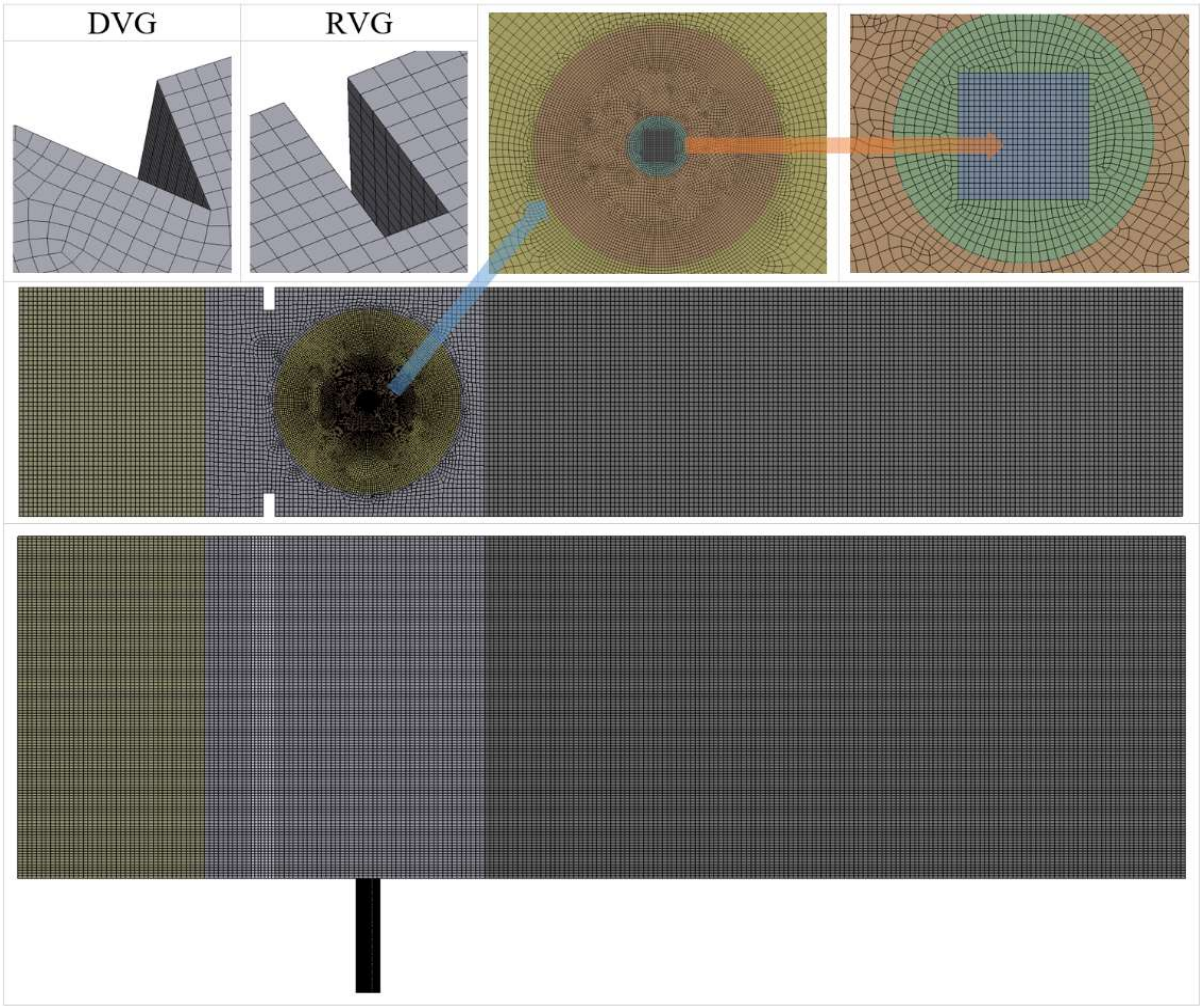

Figure 4. Grid distribution of the computational domain

It is calculated by using $\lambda_T = \sqrt{10\mu_m k/\rho_m \varepsilon}$, where μ_m , k , ρ_m and ε are the molecular viscosity, turbulence kinetic energy, density and turbulence emission rate, respectively. Figure 5. gives a detailed view of the mesh structure. As it is seen from the figure, hexahedral mesh elements were used for accurate resolving of eddies. The generated mesh models consist of 3322740 (Test 2), 3304115, 3322740, 3314240, 3327230, 3214790, 3183540 elements for the Base Channel, RVG_H10, RVG_H15, RVG_H20, DVG_H10, DVG_H15 and DVG_H20 geometric cases, respectively. The TMS values obtained from RANS simulations is about 0.36 mm for jet inlet and 0.78 mm for effective ve mixing region. Element size in the generated model is 0.38 mm for the jet inlet region and 0.82 mm for the effective mixing region.

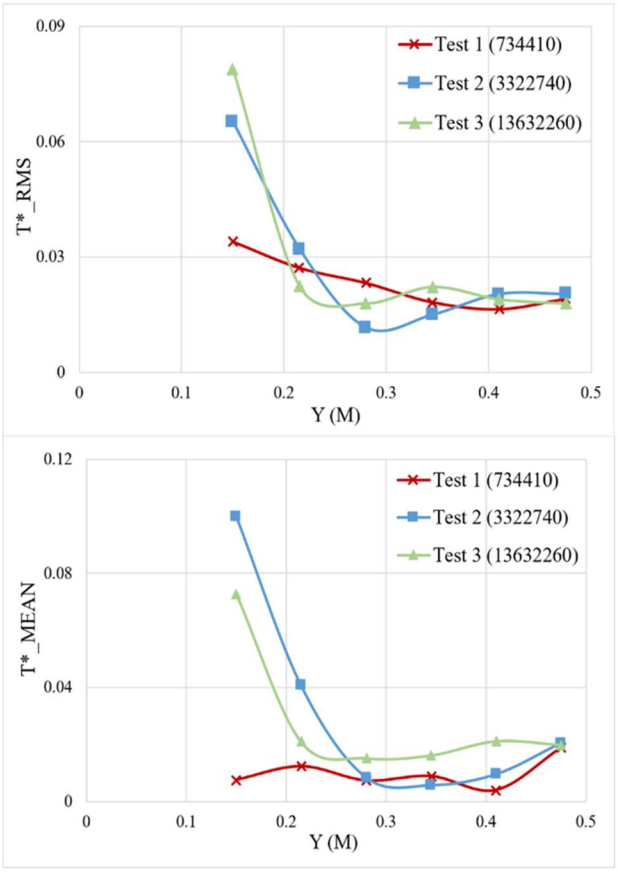

Figure 5. Mesh sensitivity analyses for Case 8 and base channel

To verify the mesh model obtained using TMS, a mesh sensitivity analysis was also performed. For this purpose, 3 test models have been formed in different element sizes. These models are Test 1, Test 2 and Test 3 with 734410, 3322740 and 13632260 element numbers, respectively. The test results shown in Figure 5 show that increasing the number of elements does not significantly change the results, but decreasing the number of elements causes a divergence.

momentum, and energy equations can be written as[25]:

$$\frac{\partial \rho}{\partial t}+\frac{\partial}{\partial x_i}(\rho \bar{u}_i)=0 \tag{3}$$

$$\frac{\partial}{\partial t}(\rho \bar{u}_i)+\frac{\partial}{\partial x_j}(\rho \bar{u}_i \bar{u}_j)=\frac{\partial \bar{\sigma}_{ij}}{\partial x_j}-\frac{\partial \bar{p}}{\partial x_i}-\frac{\partial \bar{\tau}_{ij}}{\partial x_j}+S_{M,i} \tag{4}$$

$$\frac{\partial}{\partial t}(\rho \bar{h})+\frac{\partial}{\partial x_j}(\rho \bar{h} \bar{u}_j)=\frac{\partial}{\partial x_j}\left(k_{\text{eff}}\frac{\partial \bar{T}}{\partial x_j}\right) \tag{5}$$

2.2.Numerical Method

As it is known in a turbulent flow, small vortices are absorbed into energy, while large vortices are highly influenced by geometric parameters. These properties related to turbulent flows lead researchers to solve large-scale eddies and to model small vortices using the sub-grid scale (SGS) model. The basic feature of the LES model is to filter these vortices using the Navier-Stokes equations according to the size scale. With this method, Navier-Stokers equations are filtered according to their size and the fluctuations below a certain size are modeled. Fluctuations in the filtered size are resolved. Filtration is done by a defined filtering function. Filtering function defined by;

$$G(x-x')=\begin{cases}1/\Delta, & |x-x'|\le \Delta/2\\ 0, & otherwise\end{cases} \tag{1}$$

Where Δ is the filter width. The wave length of the smallest scale is separated by the filter operator. The filter function decides the dimensions and structures of small scales. The desired variable is filtered by;

$$\bar{\phi}(x)=\int_{D_f}\phi(x')G(x-x')dx \tag{2}$$

where D_f is the fluid domain, and G is the filter function that determines the scale of the resolved eddies. After applying the filter operator, the mass conservation,

where $\bar{u}_i$, ρ, $\bar{p}$, $S_{M,i}$, $\bar{h}$ and $\bar{T}$ represent filtered velocity component, the density of fluid, filtered pressure, gravitational body force, filtered enthalpy, and temperature, respectively.

The SGS stress model derived from the filtration processes is unknown and needs to be modeled. The SGS turbulence models in FLUENT apply the Boussinesq hypothesis and are derived using the following equation.

$$\tau_{ij}-\frac{1}{3}\tau_{kk}\delta_{ij}=-2\mu_t\bar{S}_{ij} \tag{6}$$

It should be noted that Wall Adapting Local Eddy Viscosity (WALE) was used as the SGS model. This model is successfully used in modeling turbulent flows that flow through a confined channel. The swirl viscosity in the WALE model,

$$\mu_t = \rho L_s^2 \frac{(S_{ij}^d S_{ij}^d)^{3/2}}{(\overline{S}_{ij}\overline{S}_{ij})^{5/2} + (S_{ij}^d S_{ij}^d)^{5/4}} \qquad (7)$$

where S_{ij}^d is a deviatoric part of rate-of-strain tensor and L_s is the mixing length for sub-grid[25].

3. RESULTS AND DISCUSSION

Since the temperature oscillations in the mixing zone are sudden and random, it is very difficult to predict them. Therefore, such problems should be examined through a system rather than one-to-one point data. In this study, geometric and physical dynamics affecting the thermal mixing were studied extensively. For this purpose, the Mixing Index (MI) graphs, which give the thermal mixing yield in the channel, were plotted. Basically, MI graphs show how much temperature values measured in a given region deviate from the average temperature. MI is calculated by $MI = (S_T/\Delta T) \times 100$, where $S_T = \sqrt{\left(\sum_{i=1}^{n}(T_i - T_{avg})^2\right)/(n-1)}$ is the standard deviation of temperature at any measurement point. $MI = 0$ means a flat temperature profile which mean complete thermally mixed flow[26]. As shown in Figure 1, there are 64 temperature measurement points within the test channel. The temperature values are taken from these points for a flow time of 4 seconds at 0.01 second intervals. There are eight temperature measurement columns in the channel from left to right, and each column has eight measuring points. The MI graphs were obtained by using the temperature values of the measurement points in these columns. In MI graphs, the thermal mixing yield of each column is given as percentage. As the MI values approach zero, the thermal mixture performance increases and MI = 0 represents the perfect thermal mixing.

There are two points that should be considered in the analysis of the thermal mixings problems. The first is the analysis of whether or not the temperature oscillations in the system have reached the channel walls. Secondly, if these oscillations reach the channel walls, then it should be determined whether or not this creates a risk of thermal stress. The result of the Power Spectral Density (PSD) determines amplitude of oscillations. It has seen that the PSD results are not much affected by the geometric parameters in similar boundary conditions. In previous studies, we obtained numerically and experimentally that the temperature oscillations in the active mixing zone were at 5 Hz frequency under similar boundary conditions [17,18,22,23].

In order to determine whether or not the temperature oscillations reach the channel walls, it is necessary to look at the isotherms. Also, to analyze the effects of the determined operating parameters on the flow behaviors in the channel, the velocity profiles are given with the streamlines. Consequently, the effects of the VGs used in the channel on the mean pressure behaviors along the channel are discussed in the last part of the findings.

3.1.Effects vortex generator type

In the previous chapters, comprehensive evaluations were made on the effects of thermal oscillations on industrial systems. The main purpose of this study is to control the temperature oscillations occurring in the crossflow- transverse jet combination and to obtain more homogeneous thermal mixtures in the mixing zone. For this purpose, vortex generator pairs were placed in the test channel before the jet entry as shown in Fig 1. Basically, two types of VG (rectangular and triangular) were selected, and their effects in the mixing zone were discussed. In Figure 6, the effects of VG types on the thermal mixing performance are given in comparison with the basic channel using MI graphs. The right and left figures depict MI variations of 2D (H20) and D (H10) for VGs height for Case 2, respectively.

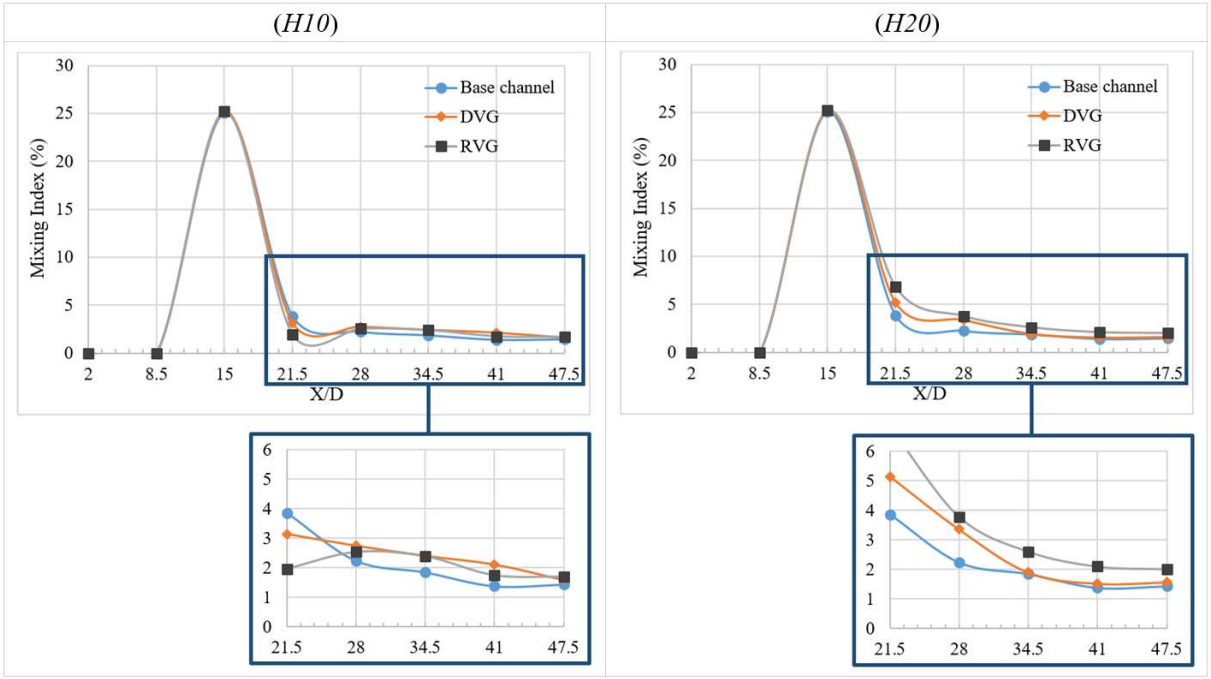

Figure 6. MI variations along the channel for Case 2 and different VG type

Interestingly, in the graphs, it is seen that the lowest MI results are in the basic channel condition in both cases. This indicates that the use of VG does not lead to an improvement in the thermal mixing as expected, but rather a relatively poor mixing performance. The lowest mix performance is seen in at low VG heights (H10) in the DVG case, and at increased VG heights (H20) in RVG case as seen from the figure from left to right, respectively. Figure 7 shows the isotherms for the same boundary conditions. As seen, in the cases where VG is used, the hot fluid is clustered in the lower half of the channel. In Figure 8, streamlines and velocity profiles are given for the same parameters of Figure 6. In this case, the fluid velocity in the mixing zone increases, especially in increasing VG height conditions (as seen in the right column). This situation partially explains the situation seen above in MI graphs.

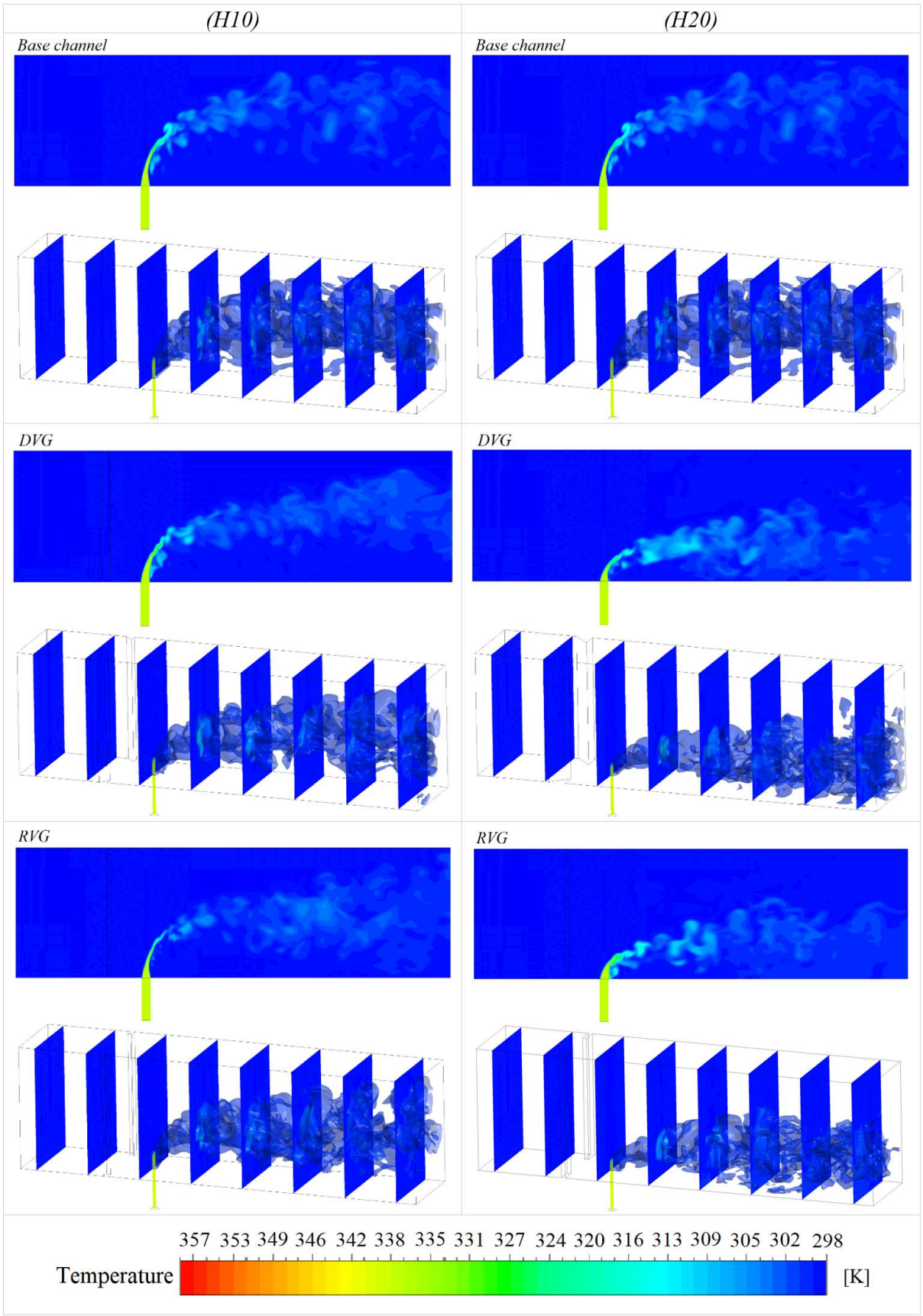

Figure 7. Isotherms for Case 2 and different VG type

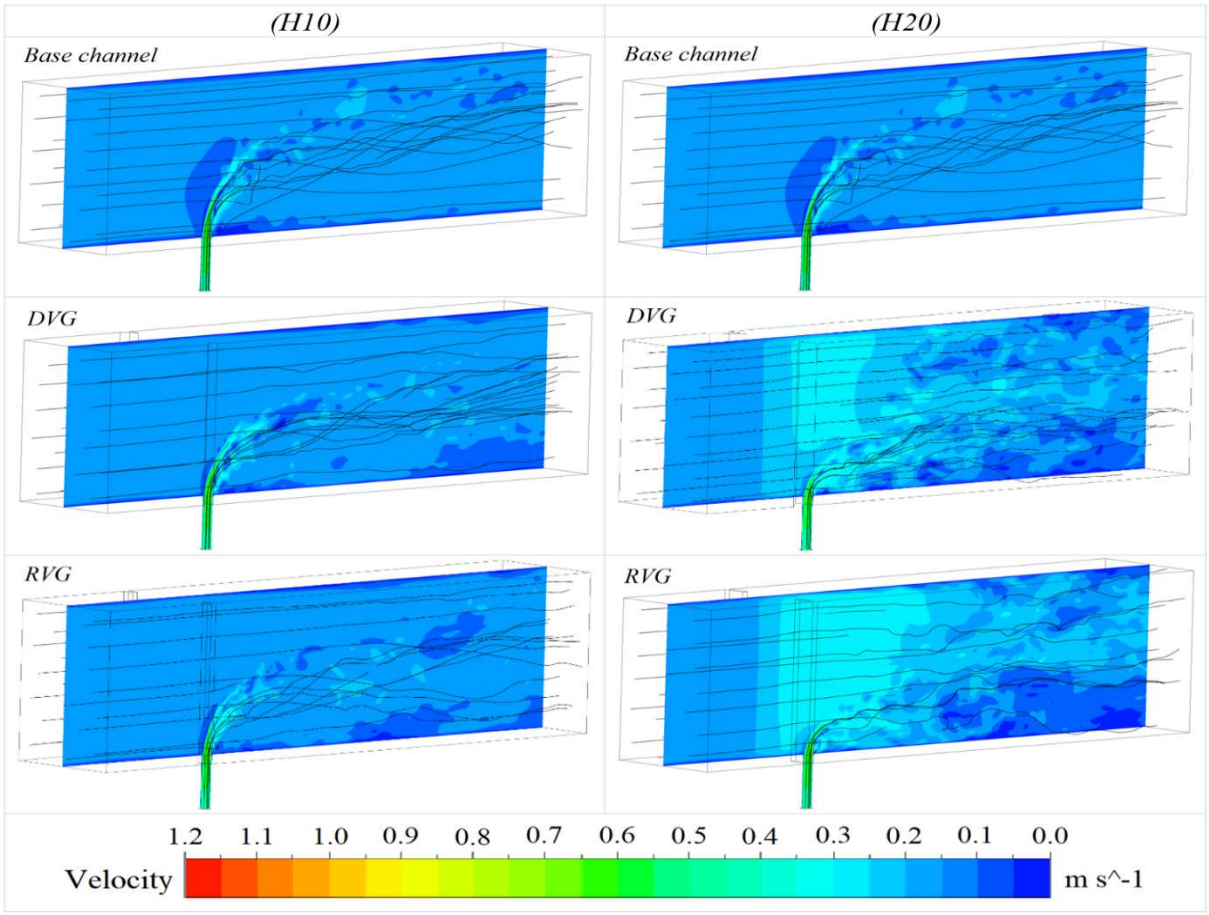

Figure 8. Streamlines and velocity profiles for Case 2 and different VG type

The increasing momentum of the fluid in the mixing zone prevents the hot fluid from being distributed throughout the channel and allows the hot fluid to clump at the bottom of the channel. Considering that the flow of the channel is turbulent as shown in Table 1, the use of VG does not create the expected vortex generation effect in the channel, but rather an extra momentum within the channel due to the narrowing section. Figure 9 shows the average pressure values along the channel for the same parameters. In parallel with the above results, with the use of VG, the fluid momentum has increased due to the narrowing section in the mixing zone and consequently, the pressure has decreased. As the VG height increases, the pressure drop in the mixing zone has increased as expected.

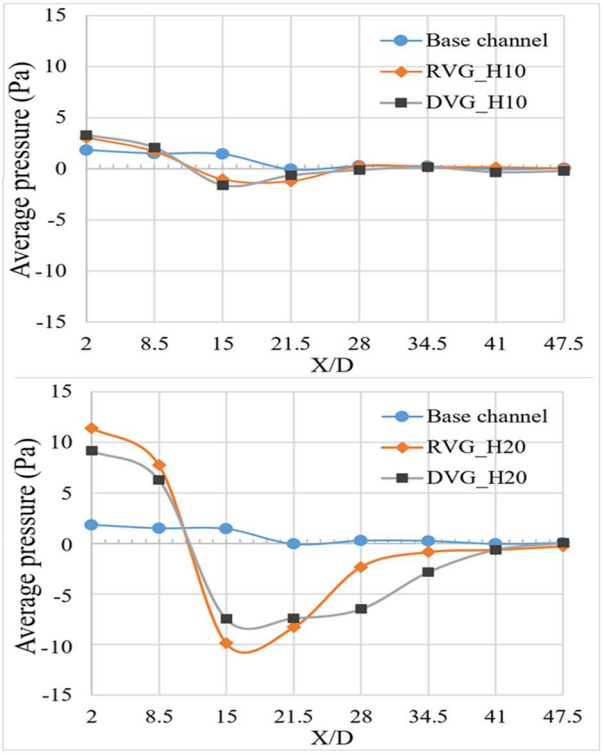

Figure 9. Average pressure along the channel for Case 2 and different VG type

1.1.Effects of vortex generator size

In this section, the height of VG pairs was selected as D (H10), 1.5D (H15) and 2D (H20), respectively, as shown in Figure 2. MI variations of different heights are given for Case 2 (left) and Case 8 (right) in Figure 10. As seen, the increased height of the VGs does not have a significant effect on the thermal mixture yield. In fact, as the VG height increases, a decrease in thermal mixing performance is observed and especially, as shown in the left figure H10 gives the best mixing efficiency. Figure 11 shows the isotherms for the same parameters. As seen, at low VG heights, the hot fluid reaches the opposite wall of the jet and causes thermal oscillations. However, as the VG height increases, due to the increased channel momentum (as seen in Figure 12), the hot fluid is shifting towards the lower regions of the channel. As can be seen from the figures, the positive effects of VGs on the thermal mixture yield cannot be mentioned. But, with the use of VG, temperature fluctuations can be removed from the duct walls. This allows VGs to can be used as a control mechanism in the systems. Figure 13 shows the average pressure changes across the channel for the same parameters of Fig 10. The situation shown here confirms the results given in Figure 12. As the VG height increases in the mixing zone, a decrease in the average pressure is observed. The use of VG gives the possibility of directing the thermal oscillations in the mixing zone. However, this situation clearly shows a pressure loss in the channel. VGs used in industrial mechanisms for controlling thermal oscillations will have an effect on the pump power used in the system. Therefore, these effects should be considered when using these tools.

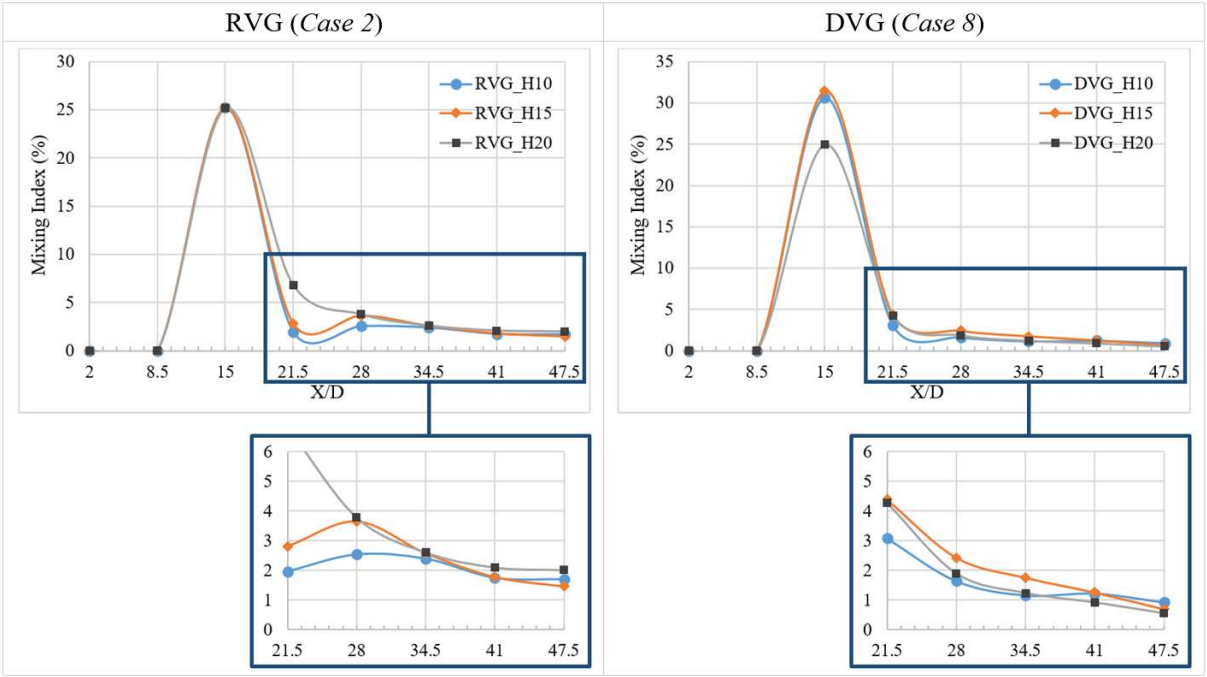

Figure 10. MI variations along the channel for different VG dimensions

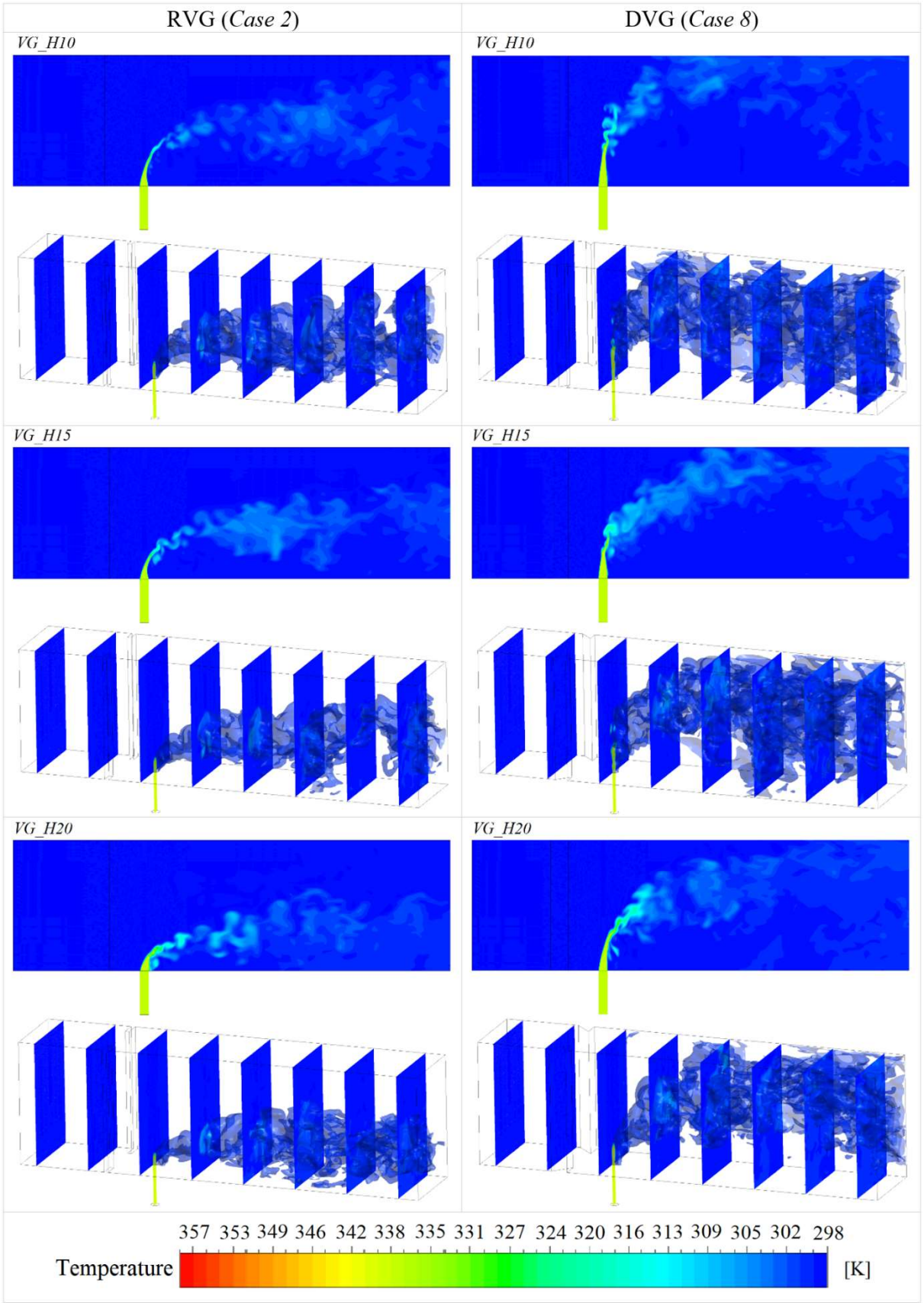

Figure 11. Isotherms for different VG dimensions

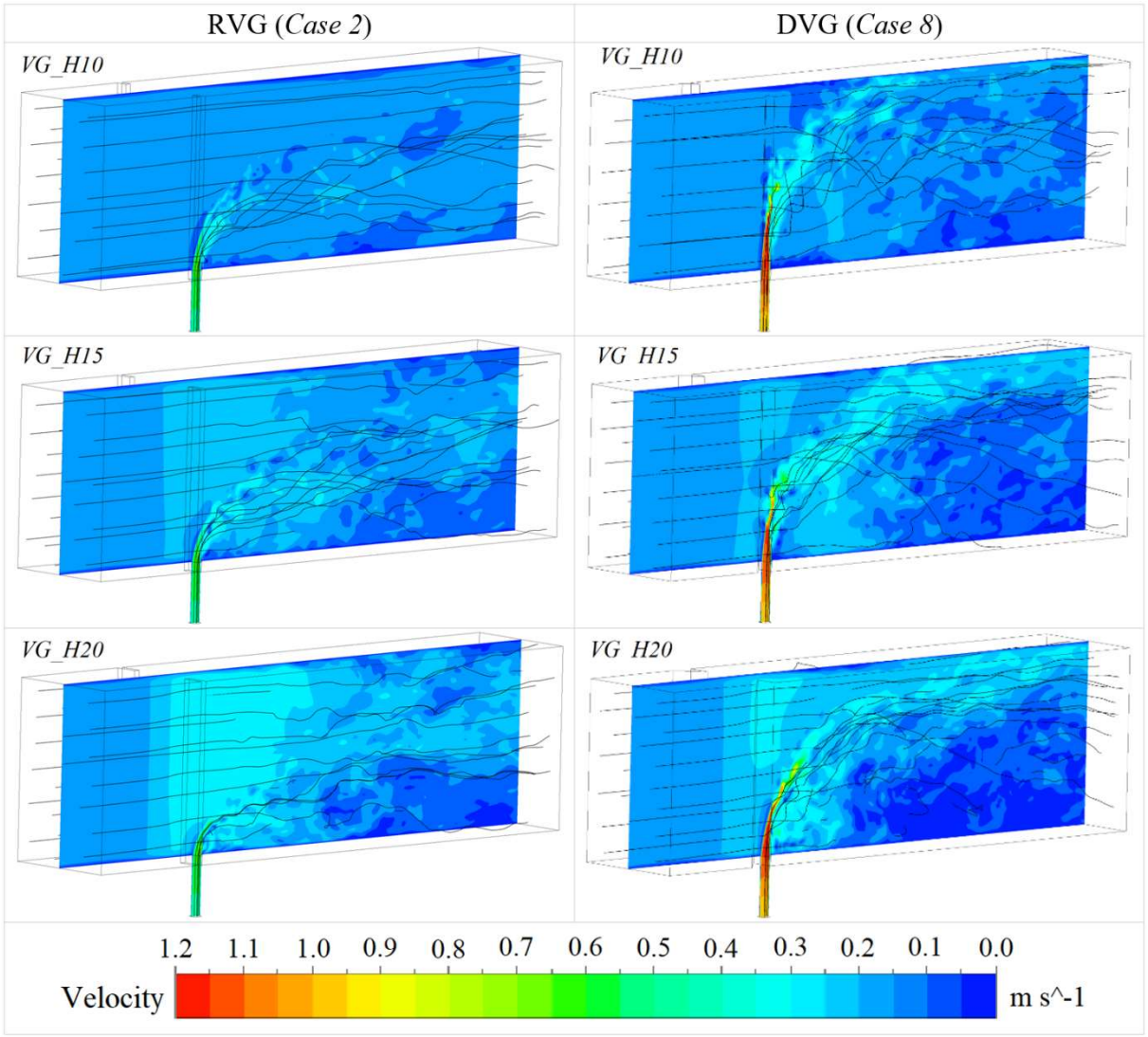

Figure 12. Streamlines and velocity profiles for different VG dimensions

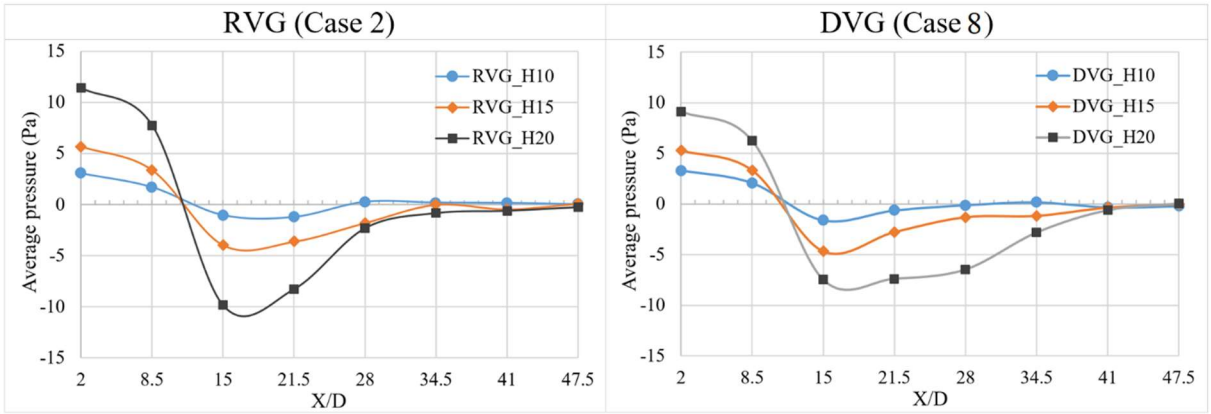

Figure 13. Average pressure along the channel for different VG dimensions

1.2.Effects of the flow rate ratio

There are nine boundary conditions in this study, as seen in Table 1. While the cross flow momentum is kept constant, the jet velocity increases gradually. This leads to the formation of three momentum ratios between the crossflow and the jet flow. Figure14 shows the effects of different momentum ratios on the MI results for DVG_H20 (left) and Base channel (right). In both cases the results are given for $\Delta T=40\ K$. In the right figure, it is seen that the best thermal mixing yield is at Uj / Uc = 5 momentum ratio when the situation related to jet inlet zone is considered. Therefore, the increasing momentum ratio in the jet inlet region did not improve the thermal mixture. However, interestingly, as seen on the left side, the effect of the momentum ratio in the jet inlet zone decreased to zero with the use of VG. As the jet momentum increases, it is clear that there is an improvement in the thermal mixture. In the continuing part of the channel, it is clear that there is an improvement in the thermal mixing as the jet momentum increases. However, as the jet velocity increases, the hot fluid reaches the channel walls and causes thermal oscillations as seen in Figure 15. It should not be noted that more hot fluid enters the channel as the momentum ratio increases. Therefore, the thermal mixing yield is expected to decrease. But, as seen in Figure 16, as the jet momentum increases, the turbulence density in the mixing zone increases and as a result, an improvement in thermal mixing performance is observed.

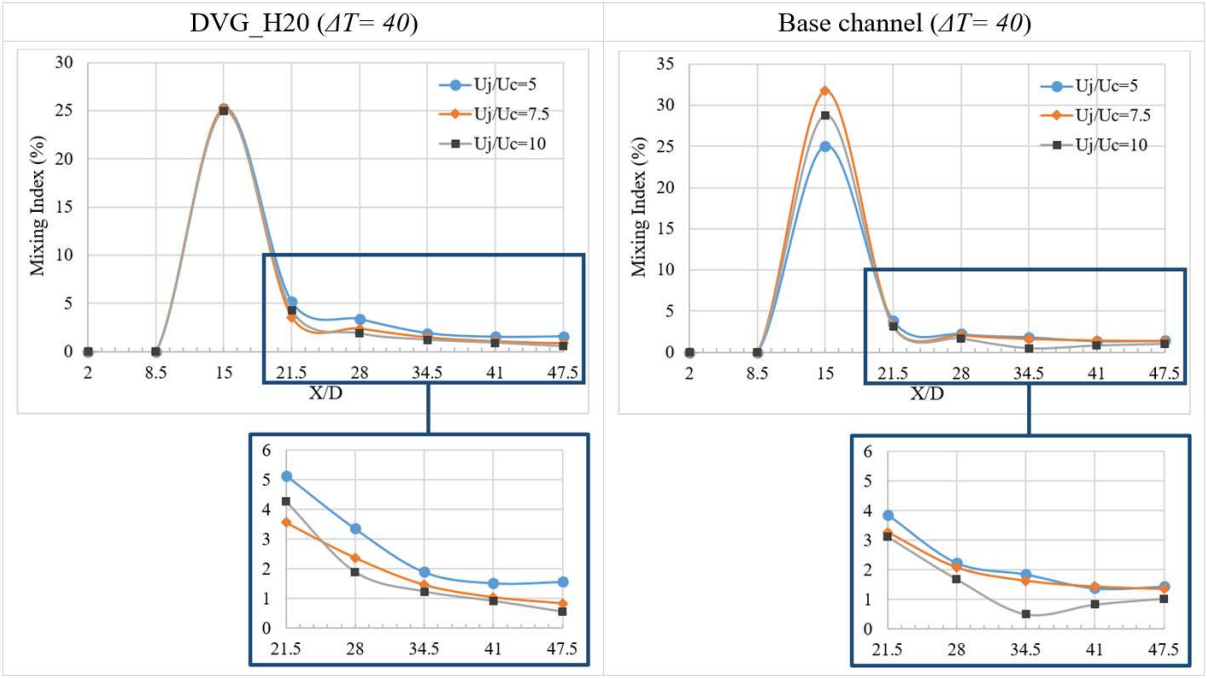

Figure 14. MI variations along the channel for different flow rate ratios

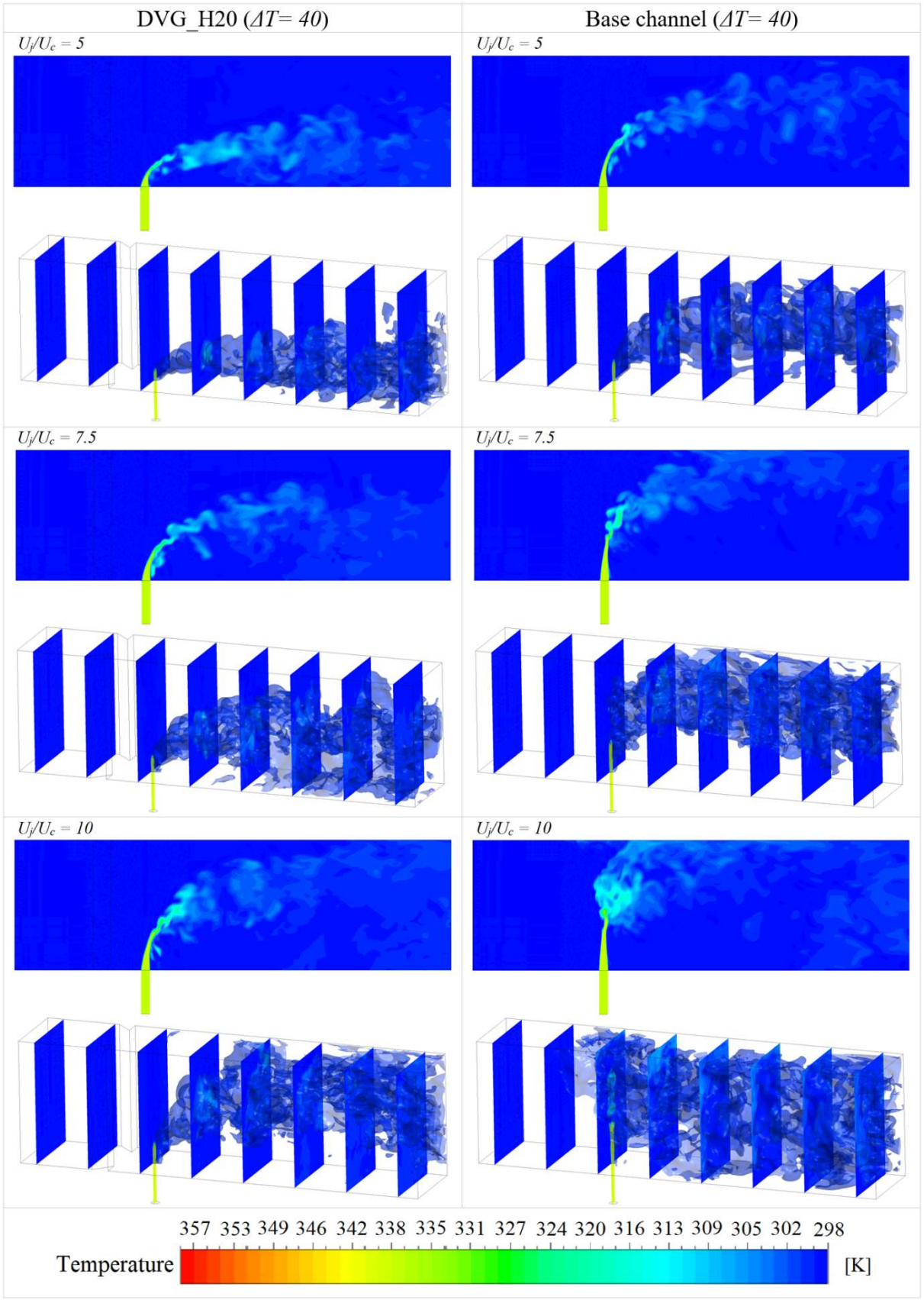

Figure 15. Isotherms for different flow rate ratios

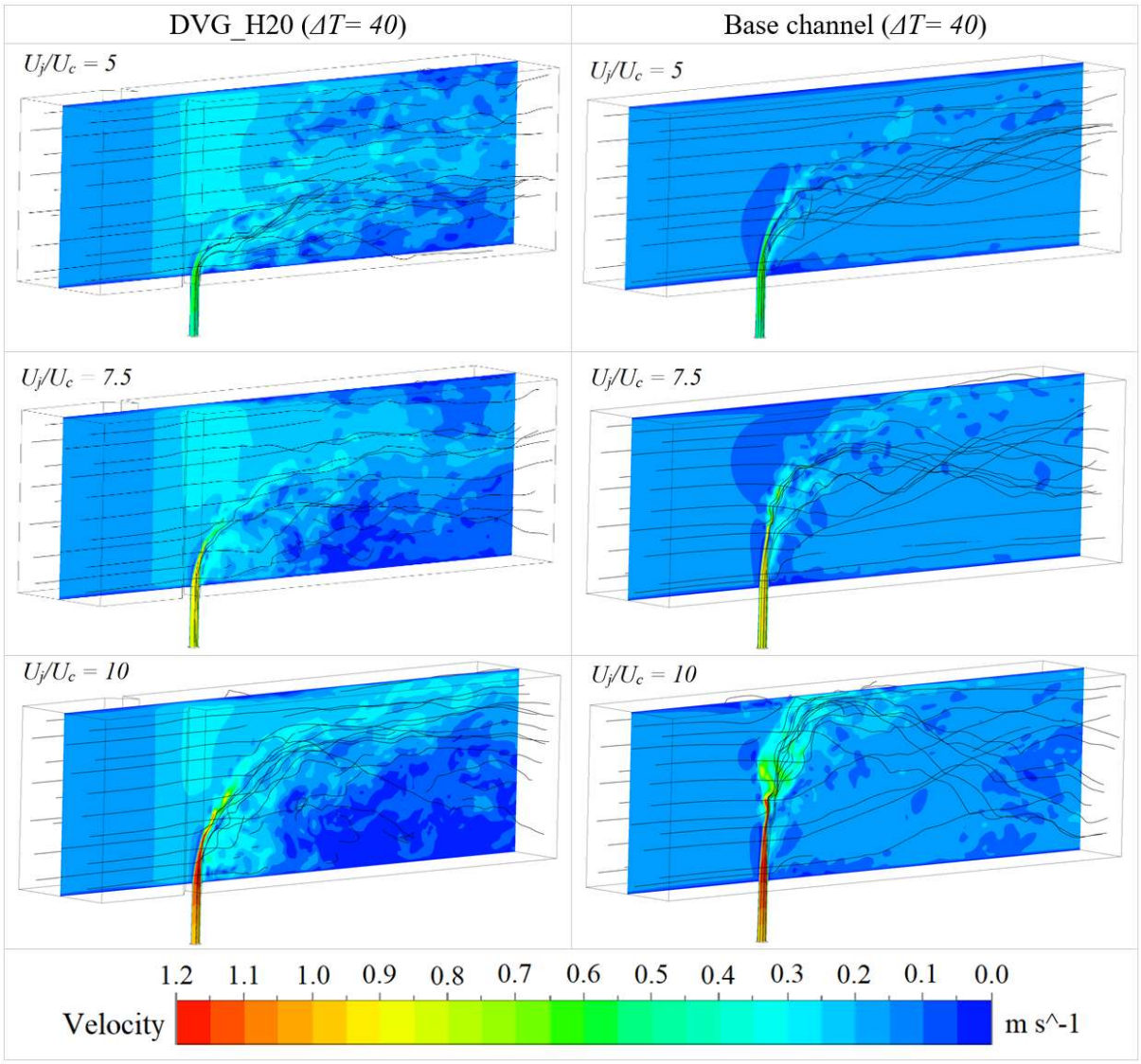

Figure 16. Streamlines and velocity profiles for different flow rate ratios

1.3.Effects of temperature difference

In this section, the effects of the temperature difference between crossflow and jet flow on thermohydraulic behaviors in the active mixing zone are discussed. As shown in Table 1, the crossflow temperature is kept constant while the jet flow temperature is gradually increased. Variations of MI for *DVG_H20* with $U_j/U_c=10$(left) and Base channel with $U_j/U_c=5$(right) are given in Figure 17. In both cases, the negative effects of increasing ΔT values on the thermal mixture yield along the channel are clearly seen. As also seen in Figure 18, as the jet temperature increases, the dominance of the hot fluid increases in the channel, and as a result, a reduction in the thermal mixture yield occurs. Figure 19 shows the streamlines and velocity profiles for the same boundary conditions. As the temperature difference rises, a relative increase is seen in the turbulence density in the mixing zone, especially on the left side, is it due to decreasing viscosity values with temperature rise.

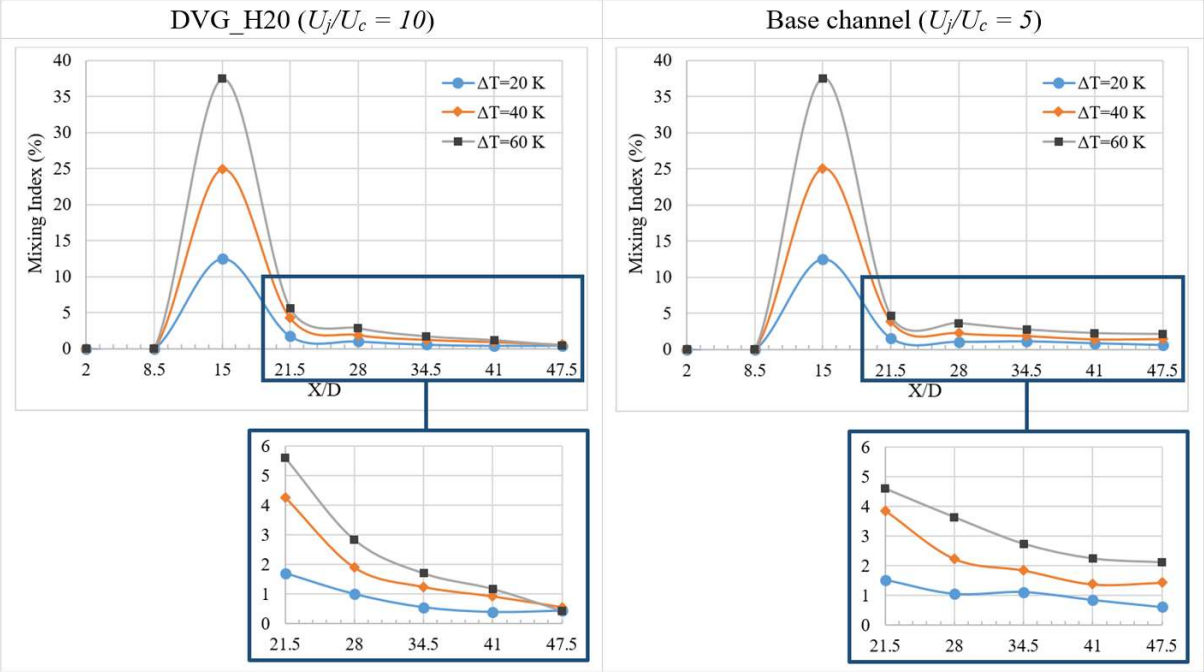

Figure 17. MI variations along the channel for different ΔT

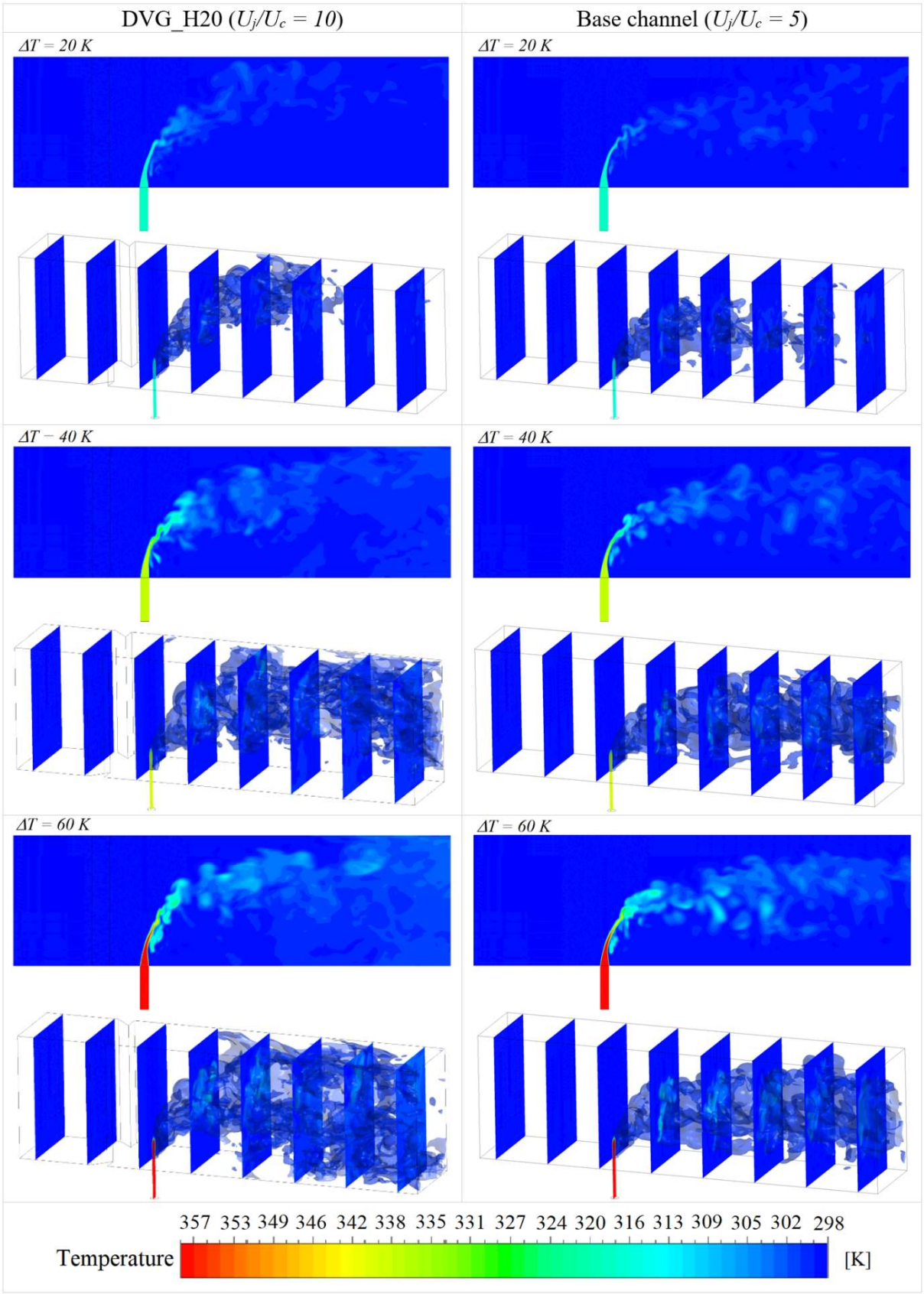

Figure 18. Isotherms for different ΔT

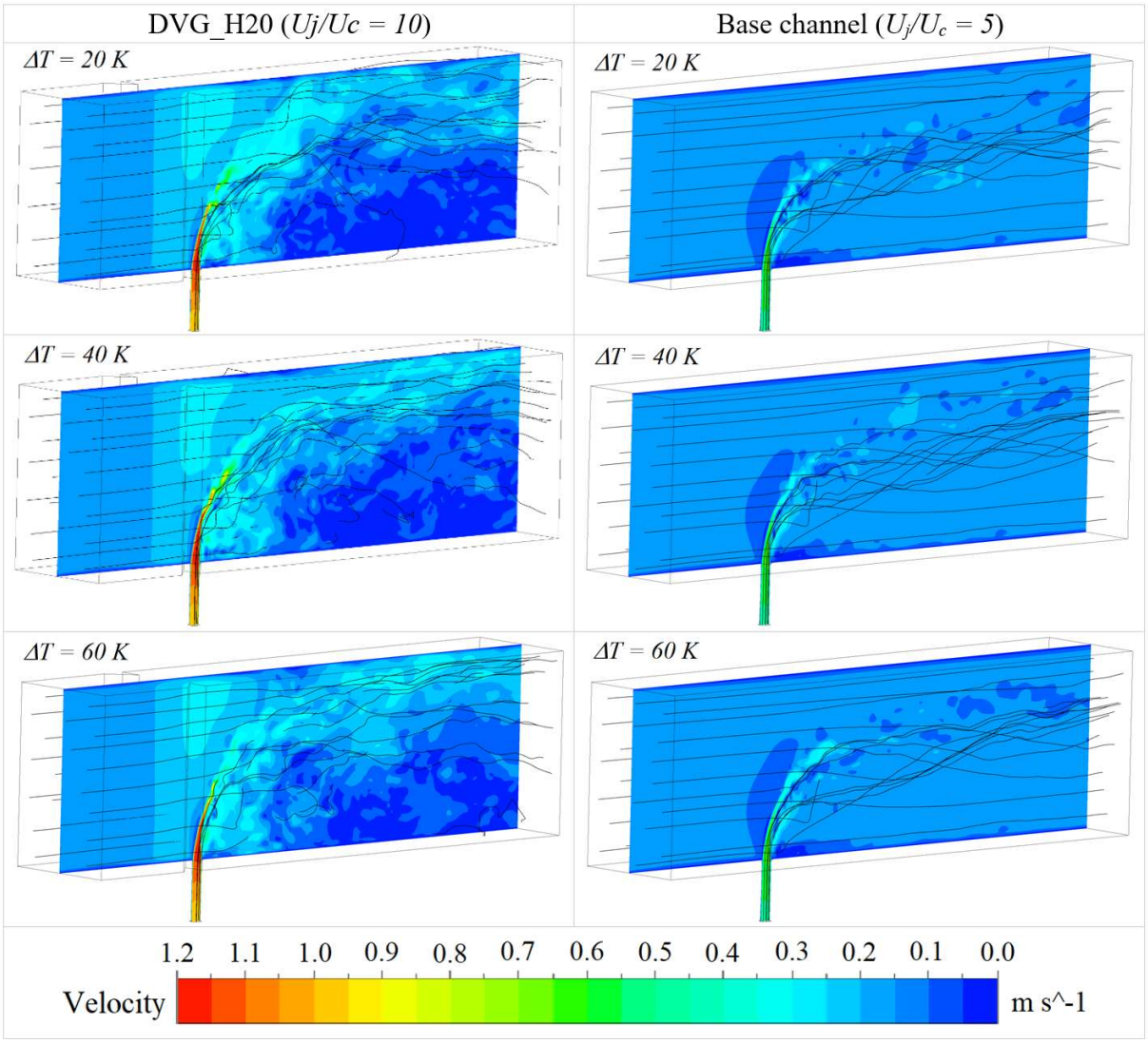

Figure 19. Streamlines and velocity profiles for different ΔT

2. CONCLUSIONS

In this study, the flow and thermal mixing characteristics of a transverse-jet flow in a crossflow channel were investigated using the LES turbulence model. Passive vortex generator (VG) pairs with different geometric properties were used to develop the fluid momentum and to control the thermal mixing performance in the test channel. In addition, nine boundary used in the analyzes. The results are discussed extensively in different aspects for four chapters.

In the first chapter, the effects of different types (rectangular and delta) VGs on the flow and thermal mixture characteristics in the active mixing zone are discussed. The results showed that the use of VG in a crossflow channel does not produce an improvement in the thermal mixing behavior, as expected. There was no significant difference between the VGs of the same height with different geometric structure in the mixture region. It is thought that the turbulence of the flow regime is significantly effective in these results. In the second part of the results, the effects of VG height are discussed. As the VG height increased, a decrease in the thermal mixing performance was observed. In some analyzes conducted without the use of VG, it was observed that the temperature oscillations reached the channel walls. It was observed that with the use of the VGs, these oscillations shifted downward from the channel walls. This divergence trend continued to increase as the VG height increased. This has led to the idea that VGs can be used as a control parameter to control thermal oscillations. However, with the use of VG, the average pressure within the

channel was reduced as expected. In the third part of the study, the effects of the momentum ratio between the crossflow and the jet flow on the thermohydraulic properties of the fluid are discussed. By keeping the cross flow rate constant, the jet velocity is gradually increased. This increases amount of hot fluid inside the duct and develops turbulence density. This development in turbulence density zone led to an increase in thermal mixing performance in the effective mixing zone. In the last part of the study, the jet temperature was gradually increased while the crossflow temperature was kept constant. This process increased the dominance of the hot water in the channel and caused a decrease in the thermal mixing performance as expected. The turbulence density was relatively increased in the mixing zone due to the reduced viscosity as the jet temperature increased.

REFERENCES

[1] International Atomic Energy Agency(IAEA), Liquid Metal Cooled Reactors: Experience in Design and Operation, Vienna, Austria, 2007.

[2] E. Sakai, T. Takahashi, H. Watanabe, "International Journal of Heat and Mass Transfer Large-eddy simulation of an inclined round jet issuing into a crossflow," *International Journal of Heat and Mass Transfer.*, Vol. 69, pp. 300–311, 2014.

[3] R. Deng, T. Setoguchi, H. Dong, "Large eddy simulation of shock vector control using bypass flow passage," *International Journal of Heat and Fluid Flow*., Vol. 62, pp. 474–481, 2016.

[4] C. Liu, Z. Wang, H. Wang, M. Sun, "Mixing characteristics of a transverse jet injection into supersonic crossflows through an expansion wall," *Acta Astronautica.,* Vol. 129, pp. 161–173, 2016.

[5] G.Y. Chuang, Y.M. Ferng, "Experimentally investigating the thermal mixing and thermal stripping characteristics in a T-junction," *Applied Thermal Engineering.,* Vol. 113, pp. 1585–1595, 2017.

[6] G.Y. Chuang, Y.M. Ferng, "Investigating effects of injection angles and velocity ratios on thermal-hydraulic behavior and thermal striping in a T-junction," *International Journal of Thermal Sciences.,* Vol. 126, pp. 74–81, 2018.

[7] A. Mcguinn, D.I. Rylatt, T.S.O. Donovan, "Heat transfer enhancement to an array of synthetic air jets by an induced crossflow," *Applied Thermal Engineering.,* Vol. 103, pp. 996–1003, 2016.

[8] C. Wang, L. Wang, B. Sundén, "International Journal of Heat and Mass Transfer A novel control of jet impingement heat transfer in cross-flow by a vortex generator pair," *International Journal of Heat and Mass Transfer.,* Vol. 88, pp. 82–90, 2015.

[9] C. Wang, L. Luo, L. Wang, B. Sundén, "International Journal of Heat and Mass Transfer Effects of vortex generators on the jet impingement heat transfer at different cross-flow Reynolds numbers," *International Journal of Heat and Mass Transfer.,* Vol. 96, pp. 278–286, 2016.

[10] D.G. Kang, H. Na, C.Y. Lee, "Detached eddy simulation of turbulent and thermal mixing in a T-junction," *Annals of Nuclear Energy.,* Vol. 124, pp. 245–256, 2019.

[11] M. Zhou, R. Kulenovic, E. Laurien, "T-junction experiments to investigate thermal-mixing pipe flow with combined measurement techniques," *Applied Thermal Engineering.,* Vol. 150, pp. 237–249, 2019.

[12] M. Kamaya, A. Nakamura, "Thermal stress analysis for fatigue damage evaluation at a mixing tee," *Nuclear Engineering and Design.,* Vol. 241, pp. 2674– 2687, 2011.

[13] J. Galpin, J.P. Simoneau, "Large Eddy Simulation of a thermal mixing tee in order to assess the thermal fatigue," *International Journal of Heat and Fluid Flow.,* Vol. 32, pp. 539–545, 2011.

[14] Y. Shao, S. Deng, Z. Wang, Y. Zhang, P. Lu, L. Zhao, W. Xu, D. Zhao, "Analysis of pressure drop in T-junction and its effect on thermodynamic cycle efficiency," *Applied Energy.,* Vol. 231, pp. 468–480, 2018.

[15] H. Ayhan, C.N. Sökmen, "CFD Modelıng of Thermal Mıxıng In T-Junctıon: Effect of Branch Pıpe Dıameter Ratıo, in: The 15th International Topical Meeting on Nuclear Reactor Thermal - Hydraulics," *NURETH-15*, Italy, p. 12. 2013.

[16] B. Kok, M. Uyar, Y. Varol, A. Koca, H.F. Oztop, "Analyzing of thermal mixing phenomena in a rectangular channel with twin jets by using artificial neural network," *Nuclear Engineering and Design.* Vol. 265, pp. 554–565, 2013.

[17] B. Kok, Y. Varol, H. Ayhan, H.F. Oztop, "Experimental and computational analysis of thermal mixing characteristics of a coaxial jet," *Experimental Thermal and Fluid Science.,* Vol. 82, pp. 276–286, 2017.

[18] B. Kok, Y. Varol, H. Ayhan, H.F. Oztop, S.G. Demiryurek, "Experimental Investigation of Thermal-Mixing Phenomena of a Coaxial Jet with Cylindrical Obstacles," *Journal of Thermophysics and Heat Transfer.,* Vol. 32, pp. 1–11, 2018.

[19] B. Kok, M. Firat, H.F. Oztop, Y. Varol, "A numerical study on thermal mixing in narrow channels inserted rectangular bodies," *International Communications in Heat and Mass Transfer.,* Vol. 44, pp. 69–76, 2013.

[20] B. Kok, Y. Varol, H.F. Oztop, A. Koca, "Analysis of thermal mixing in circle shaped body inserted inclined channel," *Experimental Thermal and Fluid Science.,*Vol. 68, pp. 1–10, 2015.

[21] Y. Varol, B. Kok, H.F. Oztop, I. Turkbay, "An experimental study on thermal mixing in a square body inserted inclined narrow channels," *International Communications in Heat and Mass Transfer.,* Vol. 39, pp. 1245–1252, 2012.

[22] Y. Varol, B. Kok, H. Ayhan, H.F. Oztop, "Experimental study and Large Eddy Simulation of thermal mixing phenomena of a parallel jet with perforated obstacles," *International Journal of Thermal Sciences.,* Vol. 111, pp. 1–17, 2017.

[23] B. Kok, Y. Varol, H. Ayhan, H.F. Oztop, "Experimental study and large Eddy simulation of a coaxial jet with perforated obstacles to control thermal mixing characteristics," *Experimental Heat Transfer.,* Vol. 31, pp. 161–182, 2018.

[24] J. Westin, F. Alavyoon, L. Andersson, P. Veber, M. Henriksson, C. Andersson, "Experiments and Unsteady CFD-Calculations of Thermal Mixing in a T-Junction, Proceedings of OECD/NEA/IAEA Workshop on the Benchmarking of CFD Codes for Application to Nuclear Reactor Safety," *CFD4NRS, Munich Germany.,* Vol. 1, pp. 1–15, 2006.

[25] I. ANSYS, ANSYS Fluent 15.0 User's Guide, ANSYS, Inc., Canonsburg, 2014. http://www.ansys.com.

[26] S.J. Wang, S. Devahastin, A.S. Mujumdar, "Effect of temperature difference on flow and mixing characteristics of laminar confined opposing jets,"*Applied Thermal Engineering.,* Vol. 26, pp. 519–529, 2006.